Available online at www.sciencedirect.com
SCIENCE DIRECT®
Journal of Magnetic Resonance 163 (2003) 105–113
JMR Journal of Magnetic Resonance
www.elsevier.com/locate/jmr

Experimental aspects of proton NMR spectroscopy in solids using phase-modulated homonuclear dipolar decoupling

Anne Lesage,[a] Dimitris Sakellariou,[b] Sabine Hediger,[a] Bénédicte Eléna,[a] Patrick Charmont,[a] Stefan Steuernagel,[c] and Lyndon Emsley[a,*]

[a] *Laboratoire de Chimie, UMR-5532 CNRS/ENS, Laboratoire de Recherche Conventionné du CEA (23V), Ecole Normale Supérieure de Lyon, 69364 Lyon, France*
[b] *Department of Chemistry, University of California, Berkeley, CA 94720, USA*
[c] *Bruker BioSpin GmbH, Silberstreifen, 76287 Rheinstetten, Germany*

Received 5 December 2002; revised 6 March 2003

Abstract

In this paper we demonstrate experimentally that the continuously phase-modulated homonuclear decoupling sequence DUMBO-1 is suitable for high-resolution proton NMR spectroscopy of rigid solids. Over a wide range of experimental conditions, we show on the model sample L-alanine as well as on small peptides that proton linewidths of less than 0.5 ppm can be obtained under DUMBO-1 decoupling. In particular the DUMBO-1 sequence yields well resolved proton spectra both at slow and fast MAS. The DUMBO-1 decoupling scheme can in principle be inserted in any multi-nuclear or multi-dimensional solid-state NMR experiment which requires a high-resolution ^{1}H dimension. An example is provided with the ^{13}C–^{1}H MAS-J-HMQC experiment.

Keywords: Solid-state proton spectroscopy; High-field NMR; Homonuclear decoupling; Fast MAS; Heteronuclear spectroscopy

1. Introduction

Proton NMR spectroscopy is widely used for the characterization of structure and dynamics in the liquid-state. Due to its high sensitivity, its high natural abundance and its ubiquitous character, the proton also constitutes an attractive nucleus to probe the structure of powdered organic materials by solid-state NMR. Thus, various NMR experiments based on high-resolution proton spectroscopy have been recently proposed to characterize the structure of complex solid compounds (for a review see [1]). For example, multi-dimensional carbon–proton correlation experiments can be applied to obtain proton chemical shift information [2–6] or to extract proton–carbon distances [7–9]. Detailed information about proton connectivities, ^{1}H–^{1}H internuclear distances, hydrogen bonds or π–π packing can be accessed by single or multiple-quantum ^{1}H homonuclear spectroscopy [10–17].

For strongly coupled systems, the success and further development of proton solid-state NMR spectroscopy relies at first on the ability to record highly resolved ^{1}H spectra. Indeed, in solids the dominant homonuclear proton–proton dipolar interactions usually lead to broad proton resonances, typically on the order of a few tens of kilohertz for static rigid organic compounds, which obscures any detail in the spectrum such as the chemical shift information. For rigid non-deuterated solids, rotation of the sample around the magic angle averages out only partially the strong dipolar couplings present among the dense proton network. Thus pure magic angle spinning (MAS) does not generally yield very high-resolution proton spectra even at the highest spinning frequencies available today [18,19]. The resolution can be further enhanced by combining rotation of the sample with the application of a homonuclear decoupling sequence that averages out the spin parts of the ^{1}H–^{1}H dipolar interactions. This is referred to as CRAMPS, for combined rotation and multiple-pulse spectroscopy [20].

* Corresponding author. Fax: +33-4-72-72-84-83.
E-mail address: Lyndon.Emsley@ens-lyon.fr (L. Emsley).

1090-7807/03/$ - see front matter © 2003 Elsevier Science (USA). All rights reserved.
doi:10.1016/S1090-7807(03)00104-6

Since the introduction of the pioneering ideas by Lee and Goldburg [21] and Waugh et al. [22], many developments have been introduced to make homonuclear decoupling sequences less sensitive to diverse experimental imperfections, and to increase decoupling performance. The first generation of homonuclear averaging techniques like WHH-4 [22], MREV-8 [23], BR-24 [24] or BLEW-12 [25] were designed for static conditions and therefore are limited to relatively slow MAS. Over the last ten years, a new generation of various improved sequences has been proposed, including frequency switched Lee–Goldburg (FSLG) [3,26–28], the semi-windowless WHH-4 sequence [29–32], the MSHOT sequences [33,34], phase modulated Lee–Goldburg (PMLG) [35–37], or the $R18_2^9$ sequence [38]. Most of these sequences work at moderately fast MAS. These new schemes together with instrumental progress in NMR spectrometers and probe technology, have led to a considerable improvement in the resolution of proton spectra. Typically, using these decoupling schemes and depending on the experimental conditions proton linewidths between 0.4 and 1 ppm can be obtained in rigid solids.

Using numerical optimization we have recently proposed a new homonuclear decoupling sequence dubbed DUMBO-1 which is based on a continuous modulation of the phase of the radiofrequency (RF) field [39]. The phase function of the DUMBO-1 sequence which was generated as a Fourier series with six coefficients (Table 1), is shown schematically in Fig. 1a. The length of the basic cycle corresponds to a 6π pulse. In the first paper, the efficiency and robustness of this sequence had been evaluated in a heteronuclear context, i.e., by observing the fine structure due to the heteronuclear carbon–proton scalar couplings on the ^{13}C spectrum of sodium acetate with DUMBO-1 decoupling applied to protons during acquisition. The objective of the work presented here is to investigate in more details the performance of this new homonuclear decoupling technique by looking directly at the resolution of DUMBO-1 decoupled proton spectra. In particular we evaluate experimentally the efficiency of DUMBO-1 as a function of the spinning frequency and B_0 magnetic field.

Table 1
Complex Fourier coefficients $c_n = a_n + ib_n$ used to define the phase of the DUMBO-1 sequence

n	a_n	B_n
1	+0.0325	+0.1310
2	+0.0189	+0.1947
3	+0.0238	+0.0194
4	+0.0107	+0.1124
5	+0.0038	−0.0456
6	−0.0013	+0.0869

The phase in 2π *units* for the mth step number in the first half of the sequence $(1 \neq m \neq 32)$ is given by $\varphi(m) = \sum_{n=1}^{6} a_n \cos(2\pi nm/M) + b_n \sin(2\pi nm/M)$, where M is the number of steps for the half of the sequence (M was set to 32 in the experiments presented in this paper). For the second half of the sequence $(33 \neq m \neq 64)$, a π phase shift is applied followed by the time reversed first half, i.e., $\varphi(m) = \varphi(2M - m) + \pi$. A constant phase can then be added to $\varphi(t)$ so that the effective field lies on the (x, z) or (y, z) plane of the rotating frame.

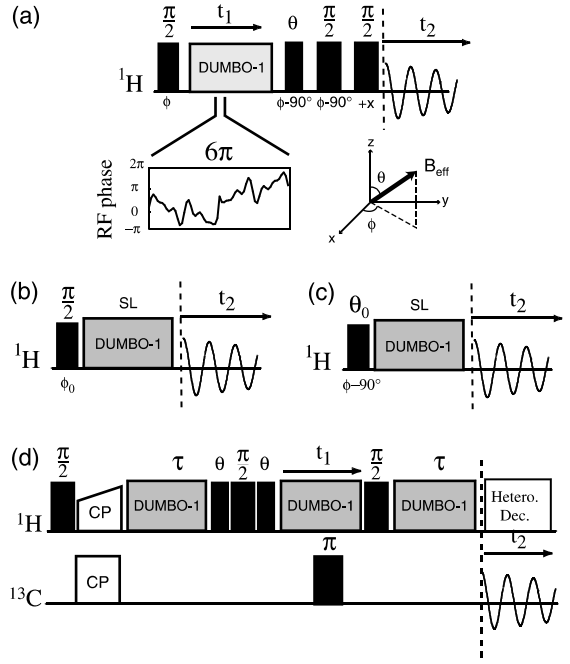

Fig. 1. (a) Pulse sequence employing DUMBO-1 decoupling for the indirect observation of high-resolution proton spectra. Quadrature detection in ω_1 is achieved using the States method [52] by incrementing the phase of the second 90° proton pulse. Detailed pulse programs and phase cycles are available on our website [53] or by request to the authors. (b) and (c) are 1D pulse sequences suitable for the determination of the angles θ and ϕ defining the orientation of the effective field present under homonuclear decoupling. The phases and pre-pulse length of the pulse sequence (a) are related to these angles. (d) MAS-J-HMQC pulse sequence [4,51] incorporating the DUMBO-1 decoupling sequence during the excitation, evolution, and reconversion periods.

2. Proton spectroscopy with DUMBO-1

2.1. Detection schemes

For proton spectroscopy, since DUMBO-1 is a windowless decoupling sequence, it should ideally be applied in the indirect dimension of a multi-dimensional homo- or heteronuclear correlation experiment. Fig. 1a shows the two-dimensional (2D) ^{1}H–^{1}H experiment allowing the indirect observation of high-resolution DUMBO-1 decoupled proton spectrum. This experiment is similar to ^{1}H–^{1}H CRAMPS-MAS experiments already proposed in the past [36,40]. The first 90° pulse creates the initial proton magnetization in a plane perpendicular to the direction of the effective field present

during the application of the DUMBO-1 decoupling sequence. During t_1, the proton magnetization evolves in the tilted transverse plane under the continuous phase-modulated decoupling sequence. At the end of the evolution time t_1, a pre-pulse of flip-angle θ is applied which rotates the proton magnetization from the tilted transverse plane to the (x, y) plane of the rotating frame. A z-filter is then applied to facilitate quadrature detection in t_1 before direct signal detection in t_2. The 2D spectrum obtained with this pulse sequence correlates the high-resolution DUMBO-1 decoupled proton spectrum in ω_1 with the pure MAS spectrum in ω_2. The one-dimensional (1D) high-resolution proton spectrum can be obtained by projection onto the ω_1 axis of the 2D spectrum, or by simply summing the ω_1 traces extracted at the various ω_2 proton frequencies.

2.2. Calibrating the effective field

The pulse phases and the pre-pulse flip angle of this experiment are related to the angles θ and ϕ defining the polar coordinates of the effective field B_{eff} present during DUMBO-1 decoupling (as illustrated schematically in Fig. 1a). Although this orientation can be determined a priori from calculations $(\theta, \phi) = (58°, 0)$, we find that the quality of spectra can be significantly improved if these parameters are determined *experimentally*. We assume that this is mainly because of imperfections that are introduced by the hardware of the spectrometer in the practical implementation of the continuously phase modulated decoupling sequence. The values of the angles θ and ϕ were determined therefore experimentally using simple 1D experiments (Figs. 1b and c, respectively). The pulse sequence of Fig. 1b consists of a 90° proton pulse with a RF phase ϕ_0 followed by a spin-lock period (typically several ms) under DUMBO-1 decoupling. When ϕ_0 corresponds exactly to the angle between the x axis and the (B_{eff}, z) plane, the proton signal is not spin-locked and is destroyed through dephasing. Thus the phase ϕ can be easily determined by finding the zero-crossing of the proton signal as illustrated in Fig. 2a. Misadjustment of this angle leads to

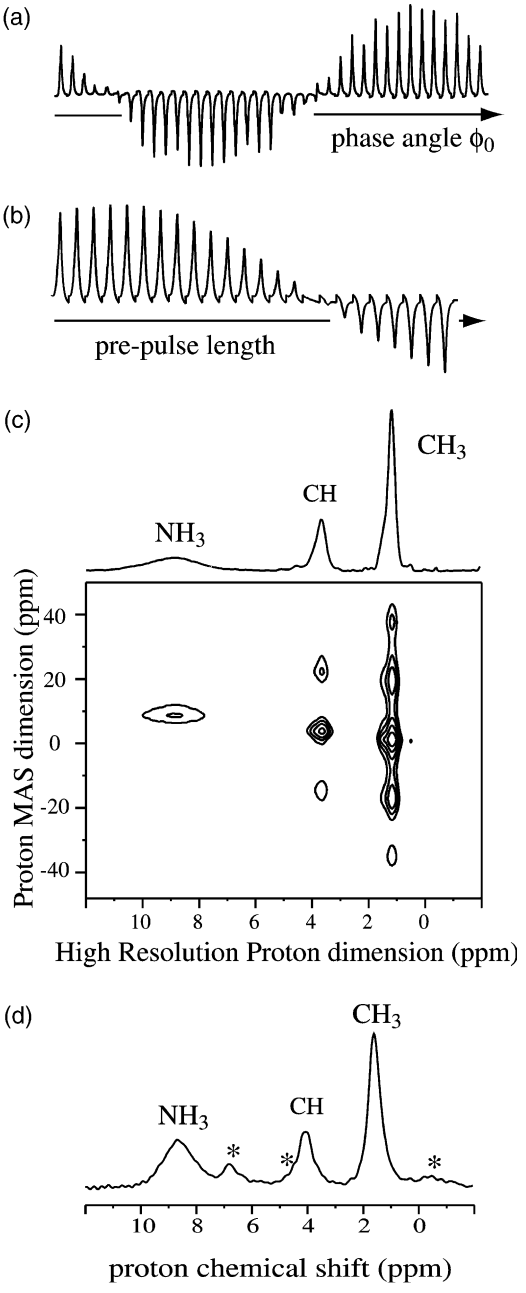

Fig. 2. (a) Intensity of the 1D proton spectrum recorded using the pulse sequence of Fig. 1b as a function of the phase ϕ_0. The phase ϕ_0 was incremented by steps of 10°. (b) Intensity of the 1D proton spectrum recorded using the pulse sequence of Fig. 1c as a function of the pre-pulse length. The pre-pulse length was varied from 0.2 to 4.8 μs by step of 0.2 μs. The (c) 2D proton–proton spectrum of a natural abundance sample of L-alanine. The experiment was performed on a Bruker DSX 500 spectrometer (proton frequency 500 MHz) using a conventional 4 mm CP MAS probe. The sample volume was restricted to about 25 μl in the center of the rotor to increase the RF field homogeneity. A total of 256 t_1 points with 16 scans each were collected. Each t_1 increment was synchronised with an integer number of DUMBO-1 cycles. As for most multiple-pulse homonuclear decoupling sequences, we observed that a small proton resonance offset (of about 2 kHz) gives a significant improvement in the resolution. A spectral width of 5555 Hz (uncorrected value) was used in the ω_1 dimension. The spinning frequency was 9 kHz. The proton RF field strength was set to 100 kHz during t_1 for DUMBO-1 decoupling. An experimental scaling factor λ_{exp} of 0.43 was calculated for this experiment. The ^{1}H spectrum shown above the 2D map was constructed by adding the three ω_1 (high-resolution proton dimension) traces extracted at the CH_3, CH, and NH_3^+ proton frequencies. No signal apodization was applied. (d) One-dimensional proton spectrum of L-alanine recorded during windowed-DUMBO-1 (8 scans) at a spinning frequency of 12 kHz and a decoupling RF field of 100 kHz. A conventional 4 mm CP MAS probe was used in this experiment. Detection windows were inserted between two DUMBO-1 cycles. The length of these detection windows was 5 μs, yielding a total cycle time of 69 μs. The signal-to-noise ratio is low because the analog filters were opened in this experiment. A scaling factor of 0.49 was measured. Stars (*) indicate quadrature images.

axial peaks in the 2D spectrum. The pulse sequence of Fig. 1c consists of a pulse of flip-angle θ_0 which brings the magnetization in the $(B_{\text{eff}},\ z)$ plane followed by a spin-lock period (typically several ms) under DUMBO-1 decoupling. When θ_0 corresponds exactly to the angle between the z axis and the effective field, all the proton magnetization is spin-locked. Thus the length of the pre-pulse can be easily determined by finding the maximum of proton signal as illustrated in Fig. 2b. Misadjustment of the length of this pre-pulse leads to quadrature images in the 2D spectrum. Note that once the value of the angle ϕ has been determined, the phase 90-ϕ can be added to all the phases of the DUMBO-1 decoupling file so that B_{eff} lies on the $(y,\ z)$ plane of the rotating frame.

The 2D spectrum of L-alanine recorded with the pulse sequence of Fig. 1a is shown in Fig. 2c. The ω_1 projection shown above the 2D map displays three well resolved peaks corresponding to the NH_3^+, CH, and CH_3 proton signals. This spectrum (as well as all the other spectra reported in this paper) was recorded using a RF decoupling field amplitude of 100 kHz, which yields a cycle time τ_c of 30 μs. Experimentally the DUMBO-1 cycle was digitized into 64 steps of 500 ns each (since each time event has to be a multiple of 50 ns on our spectrometer). Note that in all the spectra reported in this paper the proton chemical shift scales and the proton linewidths have been corrected for the corresponding experimental scaling factor (see below). In the spectrum of Fig. 2, we measured full linewidths at half height of 1060 Hz (2.12 ppm), 220 Hz (0.44 ppm), and 160 Hz (0.32 ppm) for, respectively, the NH_3^+, CH, and CH_3 proton lines (corresponding to 0.91, 0.18, and 0.13 ppm, respectively, before correction for scaling). The broadening of the amine resonance is mainly related to the interference at room temperature between the CRAMPS detection and the three-site hopping motion of the NH_3^+ group. This is a well-known phenomenon [2], that can be used to determine dynamic information under certain circumstances.

Direct proton detection using a 1D experiment is feasible if acquisition windows are inserted between DUMBO-1 cycles as reported recently for the PMLG sequence [41]. However under our experimental conditions, we found that this led to a slight decrease in proton resolution as illustrated in Fig. 2d and as expected.

3. Scaling factor of homonuclear decoupling sequences: an upper limit

The scaling factor λ_{exp} of the DUMBO-1 sequence (calculated as the ratio between the chemical shift difference between the CH_3 and NH_3^+ resonance lines in the ω_1 projection and in the fast MAS one-pulse spectrum) can be easily measured from the 2D spectrum. For the spectrum of Fig. 2c, a value of $\lambda_{\text{exp}} = 0.43$ was found, which is in reasonable agreement with the theoretical scaling factor obtained from numerical calculations ($\lambda_{\text{calc}} = 0.52$, see [39]). This scaling factor is larger than that of many existing sequences, but significantly smaller than that obtained with FSLG decoupling ($1/\sqrt{3}$, i.e., 0.57). As the spectral resolution is proportional to this scaling factor, it is important to develop homonuclear decoupling sequences that have a scaling factor as high as possible.

In the following we demonstrate for the case of static solids (or in the limit of slow MAS), that if the pulse sequence is responsible for averaging the dipolar Hamiltonian to zeroth order, the maximum scaling factor that can be obtained is $1/\sqrt{3}$. We restrict the demonstration to a two spin system, which does not alter the final result but makes it much shorter. The internal Hamiltonian of the spin system is:

$$H_{\text{int}} = \Omega_1 I_{1z} + \Omega_2 I_{2z} + d(3I_{1z}I_{2z} - \vec{I}_1 \cdot \vec{I}_2). \tag{1}$$

The RF irradiation Hamiltonian is:

$$H_{\text{rf}} = \omega_1(t)\{\cos\phi(t) I_x + \sin\phi(t) I_y\} \tag{2}$$

and this leads to a propagator for the RF that can be expressed generally as:

$$U_{\text{rf}} = U_{\text{rf}}(0,t) = \exp\{-\mathrm{i}\alpha(t) I_z\} \exp\{-\mathrm{i}\beta(t) I_y\} \times \exp\{-\mathrm{i}\gamma(t) I_z\} \tag{3}$$

where $\alpha(t)$, $\beta(t)$, and $\gamma(t)$ are time dependent Euler angles related to the $\phi(t)$ function [42–44] of the particular sequence. In an interaction frame defined by the RF irradiation, the internal Hamiltonian becomes:

$$\tilde{H}_{\text{int}} = U_{\text{rf}}^{-1} H_{\text{int}} U_{\text{rf}}. \tag{4}$$

The coefficients of the terms I_{1z} and $I_{1z}I_{2z}$ in the decomposition of $\tilde{H}_{\text{int}}$ onto the Cartesian product operator basis are found to be:

$$\mathrm{Tr}(\tilde{H}_{\text{int}} \cdot 2I_{1z}I_{2z}) = \frac{1 + 3\cos(2\beta(t))}{2}, \tag{5}$$

$$\mathrm{Tr}(\tilde{H}_{\text{int}} \cdot I_{1z}) = \Omega_1 \cos\beta(t). \tag{6}$$

Note that these results are independent of α and γ because of the invariance of the Hamiltonian to rotation around the main magnetic field z axis, and because of the irrelevance of the average phase of the time-dependent effective field. In other words, the decoupling efficiency and the scaling factor of a decoupling scheme are the same for any phase of the effective field [33].

In order to average the dipolar interaction to zero to first order for a periodic RF sequence with period t_c, the following condition is at least required:

$$\int_0^{t_c} \{1 + 3\cos[2\beta(t)]\}\,\mathrm{d}t = 0, \tag{7}$$

We can express $\cos[2\beta(t)]$ as a Fourier series:

$$\cos[2\beta(t)] = -1/3 + \sum_{n=1}^{\infty} a_n \cos(n\omega_c t), \tag{8}$$

where $\omega_c = 2\pi/t_c$. The scaling factor is the coefficient of linear I terms, say the operator I_z. Then we have:

$$\lambda = \frac{1}{t_c}\int_0^{t_c} \cos[\beta(t)]\,\mathrm{d}t = \frac{1}{t_c}\int_0^{t_c} \sqrt{\frac{1+\cos[2\beta(t)]}{2}}\,\mathrm{d}t. \tag{9}$$

Now including the constraint that the bilinear terms must, on average, be zero, we find:

$$\lambda = \frac{1}{t_c}\int_0^{t_c} \cos[\beta(t)]\,\mathrm{d}t = \frac{1}{t_c}\int_0^{t_c} \sqrt{\frac{1}{3}+\frac{1}{2}\sum_{n=1}^{\infty} a_n \cos(n\omega_c t)}\,\mathrm{d}t. \tag{10}$$

From the Schwarz inequality [45] we know that:

$$\left(\frac{1}{t_c}\int_0^{t_c} f(t)\,\mathrm{d}t\right)^2 \leqslant \frac{1}{t_c}\int_0^{t_c} f^2(t)\,\mathrm{d}t \tag{11}$$

and taking

$$f(t) = \sqrt{\frac{1}{3}+\frac{1}{2}\sum_{n=1}^{\infty} a_n \cos(n\omega_c t)},$$

we obtain:

$$\lambda^2 = \left(\frac{1}{t_c}\int_0^{t_c} \sqrt{\frac{1}{3}+\frac{1}{2}\sum_{n=1}^{\infty} a_n \cos(n\omega_c t)}\,\mathrm{d}t\right)^2 \leqslant \frac{1}{t_c}\int_0^{t_c}\left(\frac{1}{3}+\frac{1}{2}\sum_{n=1}^{\infty} a_n \cos(n\omega_c t)\right)\mathrm{d}t, \tag{12}$$

$$\lambda \leqslant \sqrt{\frac{1}{t_c}\int_0^{t_c}\frac{1}{3}\,\mathrm{d}t} = 1/\sqrt{3}. \tag{13}$$

Thus we find that: $\lambda \leqslant \sqrt{1/3}$. This means that, if the pulse sequence averages the first order of the average Hamiltonian to zero, the scaling factor cannot be greater than $1/\sqrt{3}$. Extension of this theorem to higher orders in the AHT description is in principle possible. The possibility to find larger scaling factors, and so to improve the resolution of homonuclear decoupling is an open question in the case of synchronized rotation and multiple-pulse decoupling, where the rotation alone is sufficient for the zeroth order averaging. Note that higher scaling factors than $1/\sqrt{3}$ have been found for windowed-PMLG sequences as recently reported by Vinogradov et al. [41]. However in this case the decoupling sequence does not average the dipolar couplings to zero (and indeed resolution is worse than in the windowless PMLG experiment). This effect is also observed in the windowed-DUMBO-1 spectrum of Fig. 2d, which has a higher scaling factor than normal DUMBO-1 spectra.

3.1. Spinning frequency dependence of DUMBO-1

When dealing with complex solid systems, fast MAS is often required to remove the spinning sidebands due to the chemical shift anisotropy. Thus it is of particular importance to dispose of homonuclear decoupling sequences that work well at high-spinning frequencies. In order to assess the performance of the DUMBO-1 decoupling sequence as a function of the spinning speed, we recorded a series of ^{1}H–^{1}H spectra over a wide range of MAS frequencies. Fig. 3 shows the CH and CH_3 proton resonance lines of L-alanine at spinning frequencies ranging from 10 to 30 kHz in steps of 2 kHz. For each spinning speed, the ratio τ_c/τ_r (where τ_c is the cyle time of the DUMBO-1 cycle, i.e., 32 μs and τ_r the rotor period) together with the experimental scaling factor λ_{exp} and the corrected linewidths are indicated in the table. As illustrated in Fig. 3, proton linewidths remain more or less constant and in any case smaller than 0.5 ppm up to MAS frequencies of 24 kHz (with an exception for $\omega_r = 16$ kHz, see below) whereas the intensity increases spectacularly. So far, none of the other existing decoupling schemes has been shown to give such good resolution at such high-spinning frequencies. Note that the experimental scaling factor is not affected by the spinning speed. Thus despite the fact that the DUMBO-1 decoupling scheme was first introduced to work in static and moderate MAS experiments, and in addition,

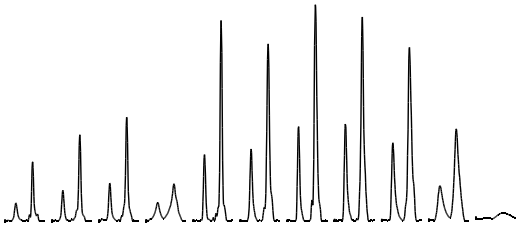

ω_r (kHz)	10	12	14	16	18	20	22	24	26	28	30
τ_c/τ_r	0.32	0.38	0.45	**0,51**	0.58	0.64	0.71	0.78	0.84	0.91	**1.06**
λ_{exp}	0.45	0.45	0.46	0.44	0.45	0.46	0.45	0.45	0.44	0.44	-
$\Delta_{(CH_3)}$ (Hz)	170	190	180	520	180	220	220	220	290	390	-
$\Delta_{(CH)}$ (Hz)	240	200	200	390	200	190	200	200	250	450	-

Fig. 3. Proton spectra of natural abundance L-alanine recorded under DUMBO-1 decoupling at different spinning frequencies. Only the CH and CH_3 resonances are shown. The experiments were performed on a Bruker DSX 500 spectrometer (proton frequency 500 MHz) using a 2.5 mm CP MAS probe. The proton spectra were constructed from 2D spectra as explained in the caption of Fig. 2. For this series of experiments, the decoupling RF field strength was set to 100 kHz and 128 t_1 increments with 16 scans each were recorded. For each spinning frequency the ratio τ_c/τ_r and the experimental scaling factor λ_{exp} are indicated in the table. The full linewidths at half height Δ are also reported for both the CH and CH_3 proton resonances (corrected values).

has quite a long cycle time (by comparison with FSLG), it shows its best decoupling performance far from the quasi-static regime and performs very well at high-spinning frequencies. It is possible that by increasing the RF decoupling power, i.e., by reducing the length of the cycle time, the curve of Fig. 3 would be shifted to the right, and that good decoupling performance could be obtained at even higher spinning frequencies. This study is under way in our laboratory.

At 16 and 30 kHz, we observe almost a complete collapse of the ^{1}H signal intensity and resolution. These two spinning frequencies correspond to a ratio τ_c/τ_r of, respectively, 1/2 and 1. These special ratios between the cycle time and rotor period are likely to correspond to strong recoupling conditions, as already observed by Filip and Hafner for the windowless WHH-4 sequence [32], or by Vinogradov et al. for the PMLG decoupling scheme [36]. These recoupling windows can be easily avoided, in particular the $\tau_c/\tau_r = 1/2$ window which seems quite sharp. Remarkably, up to a MAS frequency of 22 kHz, we observe an increase of signal intensity with increasing spinning speeds. *Between 10 and 22 kHz, more than a factor 3 is gained in signal intensity.* This effect, which, we think, has never been reported before in solids for the case of homonuclear decoupling, may be extremely relevant in experiments where the signal-to-noise ratio is a limiting factor. We remark that this effect is reminiscent of "spin tickling" type effects observed in liquids for scalar coupled spins [46,47] and in solids for heteronuclear decoupling [48]. In this latter case, it has been observed that, under certain conditions, the resonance line has a constant linewidth and increases in amplitude as the decoupling field increases. The extra intensity in the narrow centerband comes from broad decoupling sidebands which become weaker and weaker in intensity. In solids these sidebands are usually so broad as to be unobservable. In the case we observe here we therefore attribute the increase in centerband intensity to the progressive reduction of broad spinning sidebands. Preliminary numerical calculations support this hypothesis, and more detailed calculations are under way.

As mentioned previously, DUMBO-1 was originally designed to work at slow spinning frequencies, and as we have seen from Fig. 3 in practice the linewidth varies very little with spinning speed. In order to verify performance at low speeds, Fig. 4 shows the 2D proton–proton spectrum of the dipeptide Ala–Asp, recorded with a spinning speed of 2 kHz. The 1D proton spectrum shown above is well resolved with all proton resonances having linewidths of about 0.5 ppm. Additionally, at these speeds, spinning sidebands due to the proton CSA start to appear in the spectrum, as shown in Fig. 4. These sidebands could in principle be used to quantitatively determine proton CSA. In practice multi-dimensional methods involving spinning speed scaling are preferable [49], and a detailed study in this sense will be presented elsewhere.

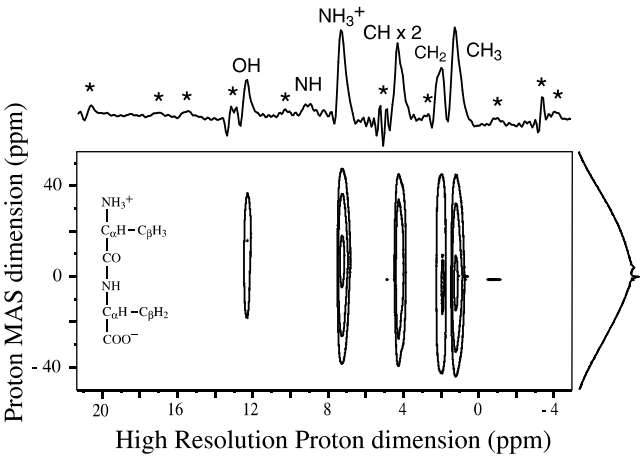

Fig. 4. DUMBO-1 decoupled proton spectra of the dipeptide Ala–Asp recorded at low spinning frequency. The spinning frequency was set to 2 kHz for this experiment. The powder sample of the dipeptide Ala–Asp was purchased from Sigma and used without further recrystallization. A total of 256 t_1 points with 16 scans each were collected. A spectral width of 8680 Hz (uncorrected value) was used in the ω_1 dimension. The proton RF field strength was set to 100 kHz during t_1 for DUMBO-1 decoupling. An experimental scaling factor λ_{exp} of 0.48 was calculated for this experiment. Corrected linewidths of 250 Hz (0.5 ppm), 265 Hz (0.53 ppm), 250 Hz (0.5 ppm), 240 Hz (0.48 ppm), and 205 Hz (0.41 ppm) were measured, respectively, for the CH_3, CH_2, CH, NH_3^+, and OH peaks. Stars indicate the axial peak and spinning sidebands.

3.2. B_0 field dependence of DUMBO-1

The performance of the DUMBO-1 decoupling scheme was evaluated experimentally at various B_0 magnetic fields on L-alanine (Figs. 5a, b, and c) and the results were compared with calculated data (Fig. 5f). An enhancement in the resolution of proton spectra can be expected when increasing the B_0 magnetic field because of the larger chemical shift dispersion in higher field and because of a more effective truncation of the dipolar couplings among protons by the increased Zeeman interaction. This tendency, which is indeed obtained for the calculated data (see Fig. 5f), was however not observed experimentally. At 750 MHz, proton linewidths at half height of 0.34 ppm were measured for the α and β protons of L-alanine which is significantly larger than the linewidths obtained at 600 MHz (0.26 and 0.28 ppm, respectively). In this series of experiments, care was taken to ensure the maximum degree of similitude, but one should note that the probe electronics are not the same at the different fields. Nevertheless it is worth pointing out that the proton linewidths observed at 750 MHz under DUMBO-1 decoupling are still significantly smaller than those obtained with pure fast MAS at this field (Fig. 5e).

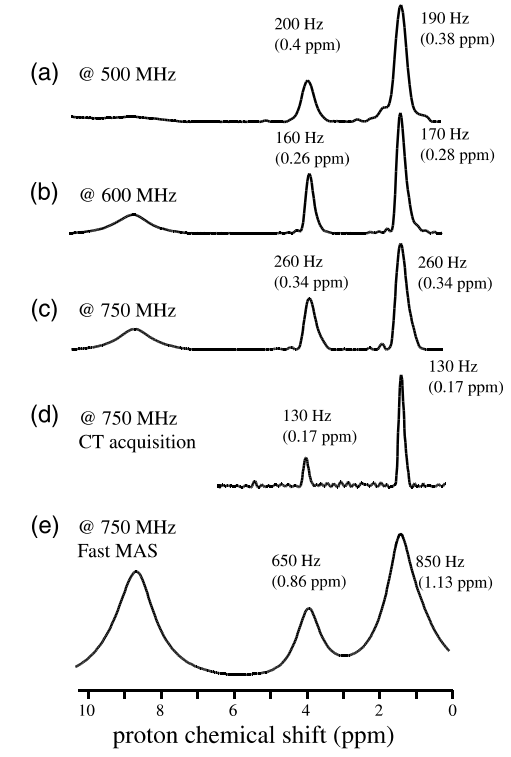

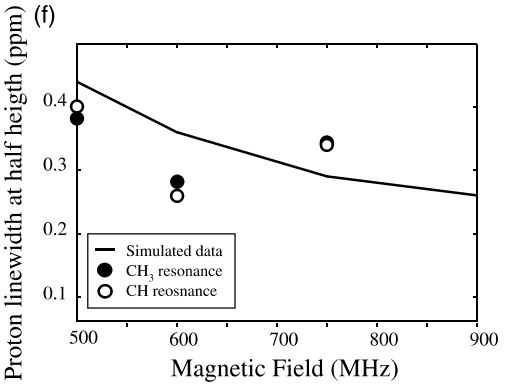

Fig. 5. Comparison between DUMBO-1 decoupled proton spectra of L-alanine recorded at various B_0 fields. Spectrum (a) was recorded under the same experimental conditions as in Fig. 3 at a spinning frequency of 12 kHz. Spectra (b) and (c) were obtained, respectively, on a Bruker DSX 600 MHz and Bruker DSX 750 MHz spectrometers using conventional 4 mm CP MAS probes at a spinning frequency of 12.5 kHz and a decoupling RF field strength of 100 kHz. The constant-time acquisition spectrum (d) was recorded using a 2D experiment as reported in [50] with a constant time $T = 16.8$ ms. The fast MAS spectrum (e) was recorded at a spinning frequency of 30 kHz with a 2.5 mm probe. For spectra (a), (b), and (c) experimental scaling factors λ_{exp} of, respectively, 0.45, 0.48, and 0.45 were measured. (f) The experimental full linewidths at half height (circles) are compared with proton linewidths obtained from numerical simulations (solid line). The simulations were done with the SIMPSON program [54] using standard methods [55]. A spin system of four protons was considered. The following parameters were used for the simulations: dipolar couplings $D_{12} = 18$ kHz, $D_{13} = 14.5$ kHz, $D_{14} = 9.5$ kHz, $D_{23} = 27.5$ kHz, $D_{34} = 14$ kHz; $D_{24} = 17$ kHz; chemical shifts: $\delta_1 = -1$ ppm, $\delta_2 = 1$ ppm, $\delta_3 = 3$ ppm, $\delta_4 = 4$ ppm; CSA (axially symmetric tensors) $\delta_1 = 2$ ppm, $\delta_2 = 10$ ppm, $\delta_3 = 2$ ppm, $\delta_4 = 4$ ppm; RF field amplitude for DUMBO-1 decoupling; $\omega_1 = 100$ kHz; MAS rotation frequency $\omega_r = 12.5$ kHz. A powder average over 440 different crystal orientations was performed to obtain the simulated spectra (not shown). The relative orientations of the CSA and dipolar tensors were chosen arbitrarily. The simulations yield a scaling factor of 0.51. For the plot, an averaged linewidth over the four proton resonances was considered (plain line).

The proton linewidths reported in this paper are by no means the limiting or "natural" proton linewidths expected in solid systems. In particular by combining a constant-time acquisition scheme with DUMBO-1 decoupling, we observed (Fig. 5d) a reduction of proton linewidths by about a factor 2 through the elimination of the contribution of the non-refocusable interactions to the apparent linewidth, in line with results previously reported for other homonuclear decoupling sequences [50].

3.3. Heteronuclear spectroscopy with DUMBO-1 decoupling

The pulse block of Fig. 1a containing the DUMBO-1 scheme can be inserted into any multi-nuclear or multi-dimensional solid-state NMR experiment which requires a high-resolution ^{1}H dimension. As an example, Fig. 6a shows the aliphatic region of the 2D MAS-J-HMQC spectrum of natural abundance Cyclosporin A (a cyclic peptide of 11 amino acids) recorded with DUMBO-1 decoupling during the excitation and reconversion periods of multiple-quantum coherences as well as during the indirect detection time t_1 (the pulse sequence is given in Fig. 1d). As reported previously [4,51], the MAS-J-HMQC spectrum gives correlations through scalar couplings between pairs of bonded protons (in ω_1) and carbons (in ω_2). The ω_1 traces (b), (c), and (d) which correspond, respectively, to a CH_3, a CH_2, and a CH group show that the proton resolution in this spectrum is about 0.5 ppm, including for the two diastereotopic protons of the CH_2 group. (CH_2 groups are the most strongly coupled groups and thus, the most difficult to decouple).

4. Conclusions

We have demonstrated experimentally that the phase-modulated DUMBO-1 ^{1}H–^{1}H homonuclear decoupling sequence is suitable for high-resolution proton solid-state NMR spectroscopy. Over a wide range of experimental conditions, an average ^{1}H resolution of about 0.4 ppm could be obtained for the aliphatic protons of the model sample L-alanine as well as for small peptides, which compares very favorably with other existing decoupling schemes. In particular, this study demonstrates

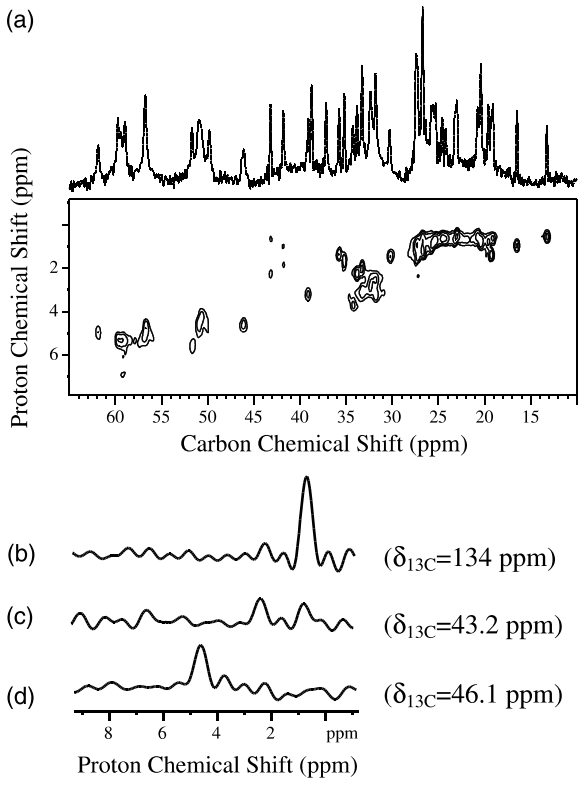

Fig. 6. (a) Two-dimensional MAS-J-HMQC spectrum of natural abundance Cyclosporin A recorded using the pulse sequence of Fig. 1d. The Cyclosporin sample was obtained from Sandoz AG and used without further recrystallization. The spinning frequency was 12 kHz. A total of 74 t_1 increments with 196 scans each were collected (10 h acquisition time). The other experimental conditions are the same as for Fig. 2. (b), (c), and (d) are three proton traces (extracted in the ω_1 dimension) corresponding to a CH_3, a CH_2, and a CH group.

that the DUMBO-1 scheme has good decoupling performance at very fast MAS. The DUMBO-1 scheme, which was previously shown to be a robust decoupling technique as regards to RF inhomogeneity [39], is easy to implement on modern spectrometers and can be inserted in any kind of multi-dimensional homo- or heteronuclear correlation experiments.

As pointed out previously, the DUMBO-1 scheme was originally developed assuming static conditions. Work is in progress in our laboratory to find phase-modulated decoupling sequences directly developed for use under fast magic-angle spinning rates. We expect that such new sequences will lead to a further enhancement of the spectral resolution of solid-state proton spectra.

Acknowledgments

We wish to thank Prof. H.J.M. de Groot and Dr. J. Hollander from Leiden University, Netherlands who welcomed us in their laboratory and gave us the opportunity to work on their 750 MHz spectrometer.

References

[1] S.P. Brown, H.W. Spiess, Advanced solid-state NMR methods for the elucidation of structure and dynamics of molecular, macromolecular, and supramolecular systems, Chem. Rev. 101 (12) (2001) 4125.
[2] A. McDermott, C.F. Ridenour, Proton measurements in biological solids, in: The Encyclopedia of NMR, Wiley, London, 1997, p. 3820.
[3] B.J. vanRossum, H. Förster, H.J.M. deGroot, High-field and high speed CP-MAS ^{13}C NMR heteronuclear dipolar-correlation spectroscopy of solids with frequency-switched Lee–Goldburg homonuclear decoupling, J. Magn. Reson. 124 (1997) 516.
[4] A. Lesage, D. Sakellariou, S. Steuernagel, L. Emsley, Carbon–proton chemical shift correlation in solid-state NMR by through-bond multiple-quantum spectroscopy, J. Am. Chem. Soc. 120 (1998) 13194.
[5] K. Saalwächter, R. Graf, H.W. Spiess, Recoupled polarization transfer heteronuclear ^{1}H–^{13}C multiple-quantum correlation in solids under ultra-fast MAS, J. Magn. Reson. 140 (1999) 471.
[6] A. Lesage, P. Charmont, S. Steuernagel, L. Emsley, Complete resonance assignment of a natural abundance solid peptide by through-bond heteronuclear correlation solid-state NMR, J. Am. Chem. Soc. 122 (2000) 9739.
[7] B.-J. vanRossum, C.P. deGroot, V. Ladizhansky, S. Vega, H.J.M. deGroot, A method for measuring heteronuclear (^{1}H–^{13}C) distances in high speed MAS NMR, J. Am. Chem. Soc. 122 (2000) 3465.
[8] K. Saalwächter, R. Graf, H.W. Spiess, Recoupled polarization-transfer methods for solid-state ^{1}H–^{13}C heteronuclear correlation in the limit of fast MAS, J. Magn. Reson. 148 (2001) 398.
[9] K. Saalwächter, H.W. Spiess, Heteronuclear ^{1}H–^{13}C multiple spin correlation in solid-state nuclear magnetic resonance: combining rotational echo double resonance recoupling and multiple-quantum spectroscopy, J. Chem. Phys. 114 (2001) 5707.
[10] U. Friedrich, I. Schnell, D.E. Demco, H.W. Spiess, Triple-quantum NMR spectroscopy in dipolar solids, Chem. Phys. Lett. 285 (1998) 49.
[11] I. Schnell, S.P. Brown, H.Y. Low, H. Ishida, H.W. Spiess, An investigation of hydrogen bonding in benzoxazine dimers by fast magic angle spinning and double-quantum ^{1}H NMR spectroscopy, J. Am. Chem. Soc. 120 (1998) 11784.
[12] S.P. Brown, I. Schnell, J.D. Brand, K. Müllen, H.W. Spiess, An investigation of π–π packing in a columnar hexabenzocoronene by fast magic-angle spinning and double-quantum ^{1}H solid state NMR spectroscopy, J. Am. Chem. Soc. 121 (1999) 6712.
[13] S.P. Brown, T. Schaller, U.P. Seelbach, F. Koziol, C. Ochsenfeld, F.-G. Kläner, H.W. Spiess, Structure and dynamics of the host–guest complex of a molecular tweezer: coupling synthesis, solid-state NMR, and quantum-chemical calculations, Angew. Chem. Int. Ed. 40 (2001) 717.
[14] S.P. Brown, X.X. Zhu, K. Saalwächter, H.W. Spiess, An investigation of hydrogen-bonding structure in bilirubin by ^{1}H double-quantum magic angle spinning solid-state NMR spectroscopy, J. Am. Chem. Soc. 123 (2001) 4275.
[15] I. Schnell, H.W. Spiess, High-resolution H-1 NMR spectroscopy in the solid state: very fast sample rotation and multiple-quantum coherences, J. Magn. Reson. 151 (2001) 153.
[16] B. Reif, C.P. Jaroniec, C.M. Rienstra, M. Hohwy, R.G. Griffin, ^{1}H–^{1}H MAS correlation spectroscopy and distance measurements in a deuterated peptide, J. Magn. Reson. 151 (2001) 320.
[17] D. Sakellariou, A. Lesage, L. Emsley, Proton–proton constraints in powdered solids from ^{1}H–^{1}H–^{1}H and ^{1}H–^{1}H–^{13}C three-dimensional NMR chemical shift correlation spectroscopy, J. Am. Chem. Soc. 123 (2001) 5604.
[18] A. Samoson, T. Tuherm, In the alpine conference on solid-state NMR: Chamonix-Mont Blanc (1999).

[19] A. Samoson, T. Tuherm, Z. Gan, High-field high speed MAS resolution enhancement on ^{1}H NMR spectroscopy of solids, Solid State NMR 20 (2001) 130.
[20] B.C. Gerstein, CRAMPS, in: The Encyclopedia of NMR, Wiley, London, 1997, p. 1501.
[21] M. Lee, W. Goldburg, Nuclear magnetic resonance line narrowing by rotating rf field, Phys. Rev. A 140 (1965) 1261.
[22] J.S. Waugh, L.M. Huber, U. Haeberlen, WHH, Phys. Rev. Lett. 20 (1968) 180.
[23] W.K. Rhim, D.D. Elleman, R.W. Vaughan, Enhanced resolution for solid state NMR, J. Chem. Phys. 59 (1973) 3740.
[24] D.P. Burum, W.K. Rhim, Analysis of multiple pulse NMR in solids, J. Chem. Phys. 71 (1979) 944.
[25] D.P. Burum, M. Linder, R.R. Ernst, Low-power multiple line narrowing in solid-state NMR, J. Magn. Reson. 44 (1981) 173.
[26] A. Bielecki, A.C. Kolbert, H.J.M. deGroot, M.H. Levitt, Frequency-switched Lee–Goldburg sequences in solids, Adv. Magn. Reson. 14 (1989) 111.
[27] A. Bielecki, A.C. Kolbert, M.H. Levitt, Frequency-switched pulse sequence: homonuclear decoupling and dilute spin NMR in solids, Chem. Phys. Lett. 155 (1989) 341.
[28] M.H. Levitt, A.C. Kolbert, A. Bielecki, D.J. Ruben, High-resolution ^{1}H NMR in solids with frequency-switched multiple-pulse sequences, Solid State NMR 2 (1993) 151.
[29] D.E. Demco, S. Hafner, R. Kimmich, J. Magn. Reson. 116 (1995) 36.
[30] S. Hafner, H.W. Spiess, Multiple-pulse line narrowing under fast magic-angle spinning, J. Magn. Reson. A 121 (1996) 160.
[31] S. Hafner, H.W. Spiess, Multiple-pulse line narrowing by fast magic-angle spinning, Solid State NMR 8 (1997) 17.
[32] C. Filip, S. Hafner, Analysis of multiple-pulse techniques under fast MAS conditions, J. Magn. Reson. 147 (2000) 250.
[33] M. Hohwy, P.V. Bower, H.J. Jakobsen, N.C. Nielsen, A high-order and broadband CRAMPS experiment using z-rotational decoupling, Chem. Phys. Lett. 273 (1997) 297.
[34] M. Hohwy, N.C. Nielsen, Elimination of high order terms in multiple pulse nuclear magnetic resonance spectroscopy: application to homonuclear decoupling in solids, J. Chem. Phys. 106 (1997) 7571.
[35] E. Vinogradov, P.H. Madhu, S. Vega, High-resolution proton solid state NMR spectroscopy by phase-modulated Lee–Goldburg experiment, Chem. Phys. Lett. 314 (1999) 443.
[36] E. Vinogradov, P.K. Madhu, S. Vega, A bimodal Floquet analysis of phase modulated Lee–Goldburg high resolution proton magic angle spinning NMR experiments, Chem. Phys. Lett. 329 (2000) 207.
[37] E. Vinogradov, P.K. Madhu, S. Vega, Phase modulated Lee–Goldburg magic angle spinning proton nuclear magnetic resonance experiments in the solid-state: a bimodal floquet theoretical treatment, J. Chem. Phys. 115 (2001) 8983.
[38] P.K. Madhu, X. Zhao, M.H. Levitt, High-resolution ^{1}H NMR in the solid-state using symmetry-based pulse sequences, Chem. Phys. Lett. 346 (2001) 142.
[39] D. Sakellariou, A. Lesage, P. Hodgkinson, L. Emsley, Homonuclear dipolar decoupling in solid-state NMR using continuous phase modulation, Chem. Phys. Lett. 319 (2000) 253.
[40] T. Schaller, A. Sebald, One and two-dimensional ^{1}H magic angle spinning experiments on hydrous silicate glasses, Solid State NMR 5 (1995) 89.
[41] E. Vinogradov, P.K. Madhu, S. Vega, Proton spectroscopy in solid state nuclear magnetic resonance with windowed phase modulated Lee–Goldburg decoupling sequences, Chem. Phys. Lett. 354 (2002) 193.
[42] J. Zhou, C. Ye, Solid State NMR 5 (1995) 213.
[43] J. Zhou, C. Ye, B.C. Sanctuary, J. Chem. Phys. 101 (1994) 6424.
[44] Y. Ishii, T. Terao, Manipulation of nuclear spin hamiltonians by rf-field modulations and its applications to observation of powder patterns under magic angle spinning, J. Chem. Phys. 109 (1998) 1366.
[45] D.R. Courant, D. Hilbert, Methods of Mathematical Physics, J. Wiley & Sons, New York, 1989, p. 49.
[46] W.A. Anderson, R. Freeman, Influence of a second radiofrequency field on high-resolution nuclear magnetic resonance spectra, J. Chem. Phys. 37 (1962) 85.
[47] R. Freeman, Double resonance, in: The Encyclopedia of NMR, Wiley, Chichester, 1997, p. 1740.
[48] J.R. Sachleben, S. Caldarelli, L. Emsley, The effect of spin decoupling on line shapes in solid-state NMR, J. Chem. Phys. 104 (1996) 2518.
[49] B. Eléna, S. Hediger, L. Emsley, Correlation of fast and slow chemical shift spinning sideband patterns under fast magic-angle spinning, J. Magn. Reson. in press (2002).
[50] A. Lesage, L. Duma, D. Sakellariou, L. Emsley, Improved resolution in proton NMR spectroscopy of powdered solids, J. Am. Chem. Soc. 123 (2001) 5747.
[51] A. Lesage, L. Emsley, Through-bond heteronuclear single-quantum correlation spectroscopy in solid-state NMR, and comparison to other through-bond and through-space experiments, J. Magn. Reson. 148 (2001) 449.
[52] D.J. States, R.A. Haberkorn, D.J. Ruben, A two-dimensional nuclear Overhauser experiment with pure absorption phase in four quadrants, J. Magn. Reson. 48 (1982) 286.
[53] http://www.ens-lyon.fr/STIM/NMR.
[54] M. Baks, R. Schultz, T. Vosegaard, N.C. Nielsen, Specification and visualization of anisotropic interaction tensors in polypeptides and numerical simulations in biological NMR, J. Magn. Reson. 154 (2002) 28.
[55] P. Hodgkinson, L. Emsley, Numerical simulation of solid-state NMR experiments, Progr. Nucl. Magn. Reson. Spectrosc. 36 (2000) 201.